SCIENTIFIC REPORTS
nature research

OPEN

Record statistics of bursts signals the onset of acceleration towards failure

Viktória Kádár[1], Gergő Pál[1,2] & Ferenc Kun[1,2*]

Forecasting the imminent catastrophic failure has a high importance for a large variety of systems from the collapse of engineering constructions, through the emergence of landslides and earthquakes, to volcanic eruptions. Failure forecast methods predict the lifetime of the system based on the time-to-failure power law of observables describing the final acceleration towards failure. We show that the statistics of records of the event series of breaking bursts, accompanying the failure process, provides a powerful tool to detect the onset of acceleration, as an early warning of the impending catastrophe. We focus on the fracture of heterogeneous materials using a fiber bundle model, which exhibits transitions between perfectly brittle, quasi-brittle, and ductile behaviors as the amount of disorder is increased. Analyzing the lifetime of record size bursts, we demonstrate that the acceleration starts at a characteristic record rank, below which record breaking slows down due to the dominance of disorder in fracturing, while above it stress redistribution gives rise to an enhanced triggering of bursts and acceleration of the dynamics. The emergence of this signal depends on the degree of disorder making both highly brittle fracture of low disorder materials, and ductile fracture of strongly disordered ones, unpredictable.

Forecasting failure is a long standing problem which has an utmost importance to mitigate the consequences of the collapse of engineering constructions and of natural catastrophes like landslides, earthquakes, volcanic eruptions, rock and snow avalanches[1–8]. Fracture processes of heterogeneous materials occurring under constant or slowly varying external loads play a decisive role for the emergence of catastrophic failures. The micro and meso-scale heterogeneity of materials has the consequence that their fracture process is accompanied by crackling noise, i.e. fracture proceeds in intermittent bursts of local breakings which generate acoustic emissions[5,9–14]. Cracking bursts can be considered as precursors of the ultimate failure of the system, so that they can be exploited to forecast the impending catastrophic event[12,15–30]. After a longer period of steady evolution, failure is approached through an acceleration of the dynamics which is indicated by the increasing rate of deformation, and acoustic or seismic signals[3,8,12,13,18,20,23,30–35]. Failure forecast methods (FFM) rely on the analogy of failure and critical phenomena which implies time-to-failure power laws of observables in the acceleration regime making possible to predict the lifetime of the system[1–3,7,8,36].

Disorder is an inherent property of natural and most of the artificially made materials. Depending on the relevant length scale, it appears in the form of dislocations, microcracks, flaws, grain boundaries, which affect the nucleation and propagation cracks. Experimental and theoretical studies have revealed that the intensity of the precursory activity, and hence, the predictability of failure, depends on the degree of materials' disorder. In the limiting case of zero disorder, the ultimate failure occurs in an abrupt way with hardly any precursors[37–40]. However, higher disorder makes possible to arrest propagating cracks giving rise to a gradual accumulation of damage with a growing rate of breaking bursts as failure is approached[18,41–43]. This effect has recently been precisely quantified by experiments performed on the compressive failure of porous glass samples where the degree of heterogeneity could be well controlled during the sample preparation[16]. It has been demonstrated that the accuracy of the lifetime prediction of FFM rapidly improves with increasing mesoscale heterogeneity of the material[16] underlining the key importance of heterogeneity for forecasting failure.

Instead of the failure time, here we focus on the onset of acceleration which marks the start of the critical regime of the evolution of the fracture process, and hence, can serve as an early warning of the imminent failure,

[1]Department of Theoretical Physics, Doctoral School of Physics, Faculty of Science and Technology, University of Debrecen, P.O.Box: 400, H-4002, Debrecen, Hungary. [2]Institute of Nuclear Research (Atomki), P.O.Box: 51, H-4001 Debrecen, Hungary. *email: ferenc.kun@science.unideb.hu

similar to the entropy change of seismicity under time reversal suggested earlier for earthquakes[25–27,44–46]. To generate fracture processes of heterogeneous materials we use a fiber bundle model[47–49], which has the advantage that varying the amount of microscale disorder, it exhibits transitions between distinct phases of perfectly brittle, quasi-brittle, and ductile fracture. To quantify how the degree of disorder determines the predictability of failure, we investigate the internal structure of the sequence of breaking bursts analyzing the record size events. Records are bursts of size greater than any previous crackling event of the fracture process so that they can easily be identified by experimental techniques both in laboratory and in field measurements above the noisy background.

The record statistics (RS) of stochastic time series has attracted a great attention due to its relevance for weather, climate and earthquake research[50–55]. The RS analysis has proven very successful to reveal trends, correlations, and spatio-temporal clustering of events in complex evolving systems[50–59]. For fracture processes, here we demonstrate that the waiting time between consecutive record breakings, i.e. the lifetime of records, is very sensitive to the details of the fracture process providing a clear signal of the acceleration of the dynamics towards ultimate failure. In particular, we show the existence of a characteristic record rank k^* which marks the onset of acceleration of record breaking: below k^* record breaking slows down due to the dominance of disorder in the fracture process, while above it the stress redistribution gives rise to an enhanced triggering of bursts after breaking events. Detecting k^* can be exploited as an early signal of the imminent ultimate failure of the system, however, the significance of the accelerating regime strongly depends on the degree of disorder. Most notably, we show that the highly brittle fracture of low disorder materials and the ductile failure of strongly disordered ones are both unpredictable due to the absence of accelerated record breaking. Our results imply the existence of a lower and upper bound of the amount of materials' disorder beyond which no meaningful failure prediction is possible.

Results

Disorder driven transition between brittle, quasi-brittle, and ductile fracture. To investigate the evolution of fracture processes leading to ultimate failure, we use a generic fiber bundle model (FBM) which has proven successful in reproducing both the constitutive response and the intermittent bursting dynamics of heterogeneous materials on the macro- and microscales, respectively[60,61]. The model is composed of N parallel fibers, similar to a rope, which have a linearly elastic behavior. Materials' disorder is represented by the random strength $\varepsilon_{th}^{i} (i = 1, \ldots, N)$ of fibers with a fat-tailed probability distribution, i.e. a power law distribution is considered

$$p(\varepsilon_{th}) = D\varepsilon_{th}^{-(1+\mu)}, \tag{1}$$

over the range $\varepsilon_{min} \leq \varepsilon_{th} \leq \varepsilon_{max}$. In the calculations the lower cutoff is fixed to $\varepsilon_{min} = 1$ so that the amount of disorder can be tuned by varying the upper cutoff ε_{max} and the exponent μ of the distribution Eq. 1, which control the range of variability of fibers's strength and the decay of weaker against stronger fibers, respectively.

The cutoff strength ε_{max} takes values in the range $\varepsilon_{min} < \varepsilon_{max} \leq +\infty$, while the disorder exponent μ is selected in the interval $0 \leq \mu < 1$. At these μ values, in the limiting case of an infinite upper cutoff $\varepsilon_{max} \to +\infty$ the disorder is so high in the system that no finite average fiber strength exists. Hence, varying the control parameters ε_{max} and μ of the model, the degree of disorder can be tuned between the extremes of zero and infinity. Computer simulations were performed by slowly increasing the external load, which generates an intermittent dynamics where fibers break in bursts analogous to acoustic outbreaks in real experiments (see Methods for further details of the model construction). The size Δ of bursts is determined as the number of fibers breaking in the correlated trail of avalanches.

It is a crucial feature of our FBM that varying the amount of disorder transitions occur between distinct phases of perfectly brittle, quasi-brittle, and ductile behaviors with qualitative differences in the macroscopic response and in the precursory bursting activity. This enables us to quantify how the degree of disorder affects the details of burst sequences and the forecastability of failure in different types of fracture. The phase diagram in Fig. 1 delineates the overall behavior of the system on the $\mu - \varepsilon_{max}$ plane based on analytical calculations (see Supplementary information (SI1) for details). The figure demonstrates that at any value of the disorder exponent in the range $0 \leq \mu < 1$, for a sufficiently low cutoff strength ε_{max} of fibers $\varepsilon_{max} < \varepsilon_{max}^{c}(\mu)$, the bundle exhibits a perfectly brittle response, i.e. a linearly elastic behavior is obtained up to the breaking of the weakest fiber which then triggers a catastrophic burst leading to an immediate abrupt failure. Above the phase boundary $\varepsilon_{max}^{c}(\mu)$ a quasi-brittle phase emerges, where global failure is approached through intermittent breaking avalanches. A representative example of the sequence of bursts up to failure can be seen in Fig. 2(a), where the size of bursts Δ is presented as a function of their order number n, similarly to the natural time analysis of time series[45,46,62]. The size of bursts Δ fluctuates due to the disorder of fibers' strength, however, the evolution of the overall structure of the sequence can be inferred: at the beginning of the fracture process the moving average of the burst size $\langle\Delta\rangle$ remains nearly constant which shows the high degree of stationarity of the crackling activity over a broad range. However, close to failure the rapidly increasing average burst size $\langle\Delta\rangle$ and the growing fluctuations of Δ indicate the acceleration of the fracture process.

This generic trend of the cracking sequence is also confirmed by the behavior of the average number a of fiber breakings triggered immediately after the breaking of a single fiber at the strain ε (for derivation see SI2)

$$a(\varepsilon) = \frac{\mu}{1 - \left(\frac{\varepsilon}{\varepsilon_{max}}\right)^{\mu}}. \tag{2}$$

The expression of $a(\varepsilon)$ has to be evaluated over the range $\varepsilon_{min} \leq \varepsilon \leq \varepsilon_c$, where ε_c denotes the critical strain $\varepsilon_c = \varepsilon_{max}/(1-\mu)^{1/\mu}$, where failure occurs. As the system approaches the critical point ε_c, the value of a

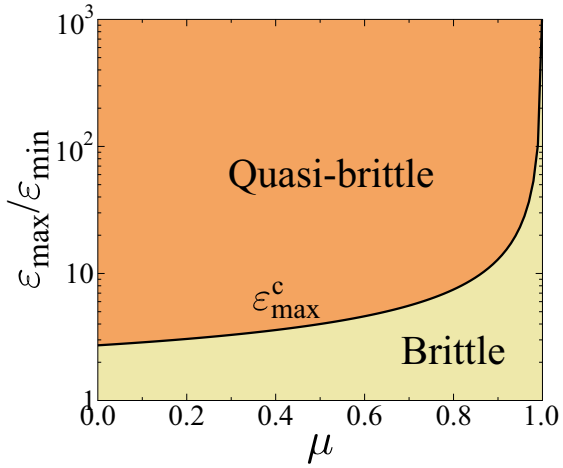

Figure 1. Phase diagram of the model on the $\mu - \varepsilon_{max}$ plane (for derivation see SI1). Increasing the amount of disorder the system undergoes brittle, quasi-brittle, or ductile fracture. The curve of $\varepsilon^c_{max}(\mu)$ gives the phase boundary between perfect brittleness and quasi-brittle fracture, while ductility is obtained in the limit $\varepsilon_{max} \to +\infty$. (GLE 4.2.5, http://glx.sourceforge.net/).

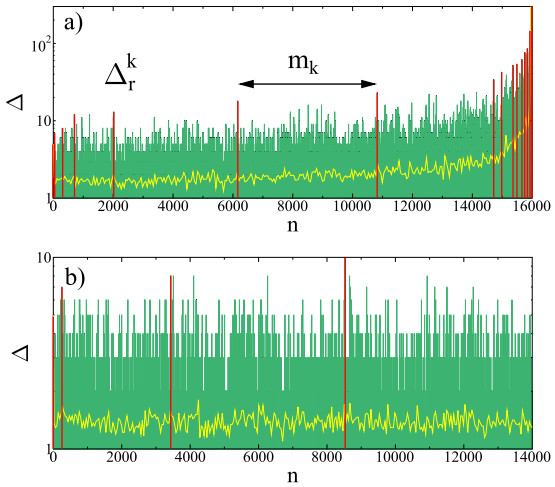

Figure 2. Event sequence of bursts, i.e. the size of bursts Δ is presented as a function of their order number n for two values of the cutoff strength (**a**) $\varepsilon_{max} = 100$, and (**b**) $\varepsilon_{max} = +\infty$ at the disorder exponent $\mu = 0.8$ in a small system of $N = 10^5$ fibers. The yellow line indicates the moving average of burst sizes $\langle\Delta\rangle$ calculated over 50 consecutive events, while the red bars highlight record size events of the series. The definition of the record size Δ^k_r and the waiting time m_k between records is also illustrated. (GLE 4.2.5, http://glx.sourceforge.net/).

monotonically increases to 1 indicating the acceleration of the fracture process and the instability emerging at the critical point. Ultimate failure occurs in the form of a catastrophic avalanche $a \geq 1$, where all the remaining intact fibers break in one event. Varying the control parameters ε_{max} and μ inside the quasi-brittle phase, the qualitative structure of the event series remains the same, however, the extension of the accelerating regime and the magnitude of acceleration, which are essential features for forecasting, are changing. The overall behaviour of the sequence of crackling events of our model has a nice qualitative agreement with the accelerating acoustic and seismic activity accompanying the creep rupture[5,13,63–65] and compressive failure[12,16,30,34] of various types of disordered materials, and the failure phenomena of geosystems such as volcanic eruptions[8,66], cliff collapse[21], breakoff of hanging glaciers[67], and landslides[23,33].

Our system has the remarkable feature that in the limit of very high disorder $\varepsilon_{max} \to +\infty$, the acceleration of the dynamics disappears $a = \mu$, and the entire series of crackling events remains stationary until the last avalanche. Figure 2(b) illustrates that the stability of the failure process is retained until the end, and no catastrophic avalanche emerges, hence, this type of fracture process is considered to be ductile in the model. The underlying mechanism is that due to the slow decay of the fat-tailed distribution of fibers' strength Eq. (1), there are sufficiently strong fibers in the bundle which can always stabilize the fracture process. Note that for $\mu > 1$ the system always undergoes perfectly brittle fracture at any cutoff strength ε_{max} (see Fig. 1).

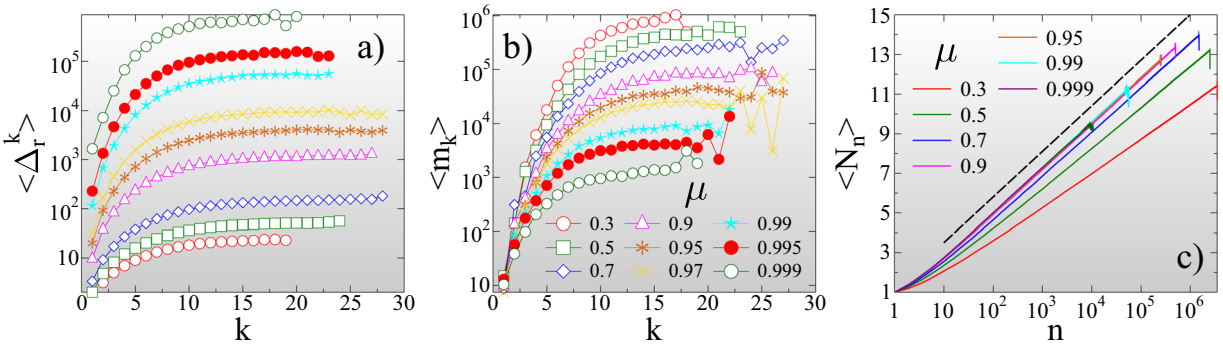

Figure 3. Average size $\langle \Delta_r^k \rangle$ (**a**) and lifetime $\langle m_k \rangle$ (**b**) of records as a function of their rank k for several values of the disorder exponent μ at an infinite cutoff strength $\varepsilon = +\infty$. (**c**) The average number of records $\langle N_n \rangle$ that occurred until n bursts are generated during the fracture process. The dashed line represents a logarithmic function. (GLE 4.2.5, http://glx.sourceforge.net/).

This powerful model allows us to unveil how the changing degree of disorder affects the predictability of the ultimate failure of the system. In the limiting case of perfectly brittle fracture, the system collapses when its load reaches the strength of the weakest fiber. Since it is not known a priori, the failure point has a great uncertainty. In the ductile phase of high disorder, the stationary bursting activity does not provide any hint of the imminent failure. Tuning the amount of disorder by varying μ and ε_{max}, we can drive the system between these two limits giving a precise quantitative characterization of the strength of acceleration of the precursory activity, and hence, the forecastability of failure. Instead of the time of ultimate failure, we focus on the onset of acceleration, analyzing the statistics of record size events of the crackling sequence.

Approaching failure through record breaking bursts. A record of crackling noise is a burst which has a size Δ_r greater than any previous event, similarly to sports like athletics, where records are the best results of a discipline[68]. Assuming that the first burst is a record, record breaking (RB) events form a monotonically increasing sub-sequence during the fracture process, as it is illustrated in Fig. 2. RB events are identified by their rank $k = 1, 2, \ldots$, which occurred as the n_kth event of the complete sequence with size Δ_r^k. As fracture proceeds, records get broken after a certain number of bursts giving rise to new records. The number of events, one has to wait to break the kth record, defines the waiting time m_k

$$m_k = n_{k+1} - n_k, \tag{3}$$

which can also be considered as the lifetime of the record. The definition of the record characteristics Δ_r^k and m_k is illustrated in Fig. 2(a). It can be observed that in the accelerating regime of the quasi-brittle fracture process in Fig. 2(a), records rapidly follow each other reaching the total number $N_n^{tot} = 22$, while in the stationary burst sequence of ductile failure in Fig. 2(b) the value of N_n^{tot} remains significantly lower ($N_n^{tot} = 4$), although the total number of events fall close to each other in the two cases. These small subsets of RB events grasp key aspects of the dynamics of fracture, namely, the acceleration of fracturing towards failure is accompanied by an accelerated record breaking indicated by the decreasing waiting time m_k in Fig. 2(a). However, in the stationary regime of the beginning of the fracture process, record breaking slows down with increasing values of m_k, similarly to ductile fracture in Fig. 2(b). To quantify these important trends and correlations in burst sequences, we analyze the statistics of the size and lifetime of records, and their evolution with the record rank as the system approaches failure at different degrees of disorder.

Record statistics in the limit of high disorder. Figure 3 demonstrates that in ductile fracture $\varepsilon_{max} = +\infty$ the statistics of records is entirely consistent with the behavior of sequences of independent identically distributed (IID) random variables[55,56]: The average record size $\langle \Delta_r^k \rangle$ is of course a monotonically increasing function of the record rank $k = 1, 2, \ldots$ for all values of the disorder exponent μ (Fig. 3(a)).

The average lifetime of records $\langle m_k \rangle$ also increases with k, since it gets more and more difficult to break the growing records of a stationary sequence (Fig. 3(b)). It follows that as fracture proceeds, the number of records N_n slowly increases with the total number of bursts n. For IID sequences a universal logarithmic dependence has been derived for the average number of records $\langle N_n \rangle$ that occurred until the nth event of the sequence[55]. Figure 3(c) shows that the IID result perfectly describes the record breaking process of ductile fracture

$$\langle N_n \rangle \approx A + B \ln n, \tag{4}$$

with the additional feature that the multiplication factor B of the logarithmic term depends on μ. Reducing the amount of disorder in the ductile phase by increasing the exponent μ towards the critical point of perfectly brittle failure $\mu \to \mu_c(\varepsilon_{max}^c = +\infty) = 1$, the qualitative behavior of the curves in Fig. 3 remains the same, however, record breaking accelerates: the asymptotic value of the record size in Fig. 3(a) rapidly increases, while the asymptotic record lifetime in Fig. 3(b) tends to zero as μ approaches 1. We quantified this behavior by calculating the

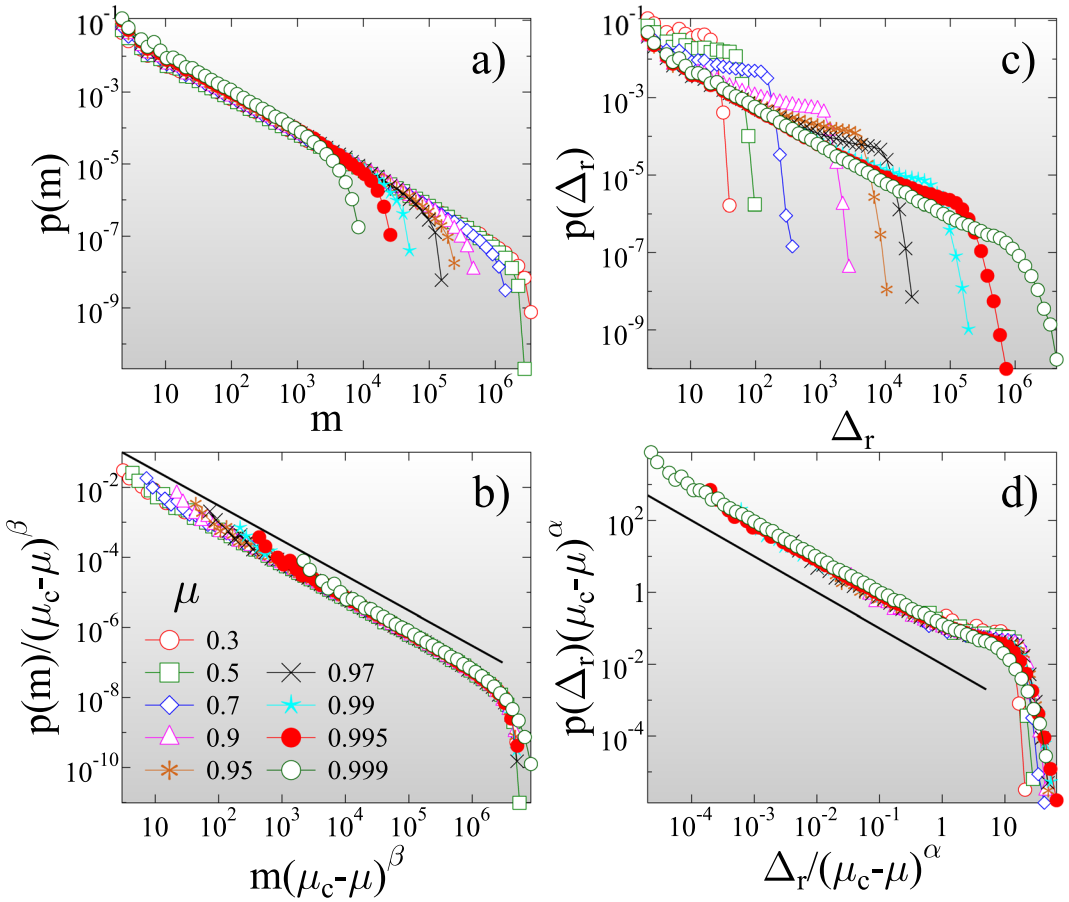

Figure 4. Probability distribution of the lifetime $p(m)$ (**a**) and size $p(\Delta_r)$ (**c**) of records for several values of the disorder exponent μ at $\varepsilon = +\infty$. Rescaling the distributions with proper powers α and β of the distance from the critical point $1 - \mu$, distributions obtained at different μ values can be collapsed on a master curve. In (**b**,**d**) the straight lines represent power laws of exponent $z = 1$ and $\tau_r = 1$, respectively. The legend is presented in (**b**) for all the figures. (GLE 4.2.5, http://glx.sourceforge.net/).

average value of the largest record size $\langle \Delta_r^{max} \rangle$ and largest waiting time $\langle m^{max} \rangle$ that occurred up to failure as function of μ. Both quantities proved to have a power law dependence on the distance from the critical point

$$\langle \Delta_r^{max} \rangle \sim (\mu_c - \mu)^{-\alpha}, \quad \langle m^{max} \rangle \sim (\mu_c - \mu)^{\beta}, \tag{5}$$

with the critical exponents $\alpha = 1.8 \pm 0.05$ and $\beta = 1.0 \pm 0.05$ (for figure see SI3). The acceleration of record breaking has also the consequence that the number of records $\langle N_n \rangle$ grows faster with the event number n for higher μ, i.e. the multiplication factor B in Eq. 4 increases to 1 as μ approaches $\mu_c = 1$ but the IID nature of the event series is retained. The IID behavior is also confirmed by the overall statistics of the lifetime m of records. The probability distribution $p(m)$ of the record lifetime m has a power law functional form

$$p(m) \sim m^{-z}, \tag{6}$$

with an exponent z, which has a universal value $z = 1$ equal to its IID counterpart[55,56] (see Fig. 4(a)). For the size distribution of records $p(\Delta_r)$ a non-universal behavior is expected in the sense that $p(\Delta_r)$ depends on the underlying distribution of burst sizes[55,56]. In our system a power law distribution is obtained

$$p(\Delta_r) \sim \Delta_r^{-\tau_r}, \tag{7}$$

with an exponent $\tau_r = 1$, which does not depend on the value of μ (see Fig. 4(c)). It is important to emphasize that approaching the critical point of brittle failure the cutoff of the size distributions $p(\Delta_r)$ diverges, while the one of the lifetime distribution $p(m)$ tends to zero, in agreement with the behavior of the high rank limit of the average size and lifetime of records in Fig. 3(a,b). Figure 4(b,d) demonstrate that rescaling the distributions $p(\Delta_r)$ and $p(m)$ according to the scaling laws Eq. 5, the curves obtained at different μ exponents can be collapsed on the top of each other. The good quality data collapse confirms the consistency of the results.

The excellent agreement of the record statistics of the burst sequence of ductile fracture with the behavior of IID sequences implies that, in spite of the increasing external load on the bundle, the entire fracture process is controlled by the microscale disorder of the system.

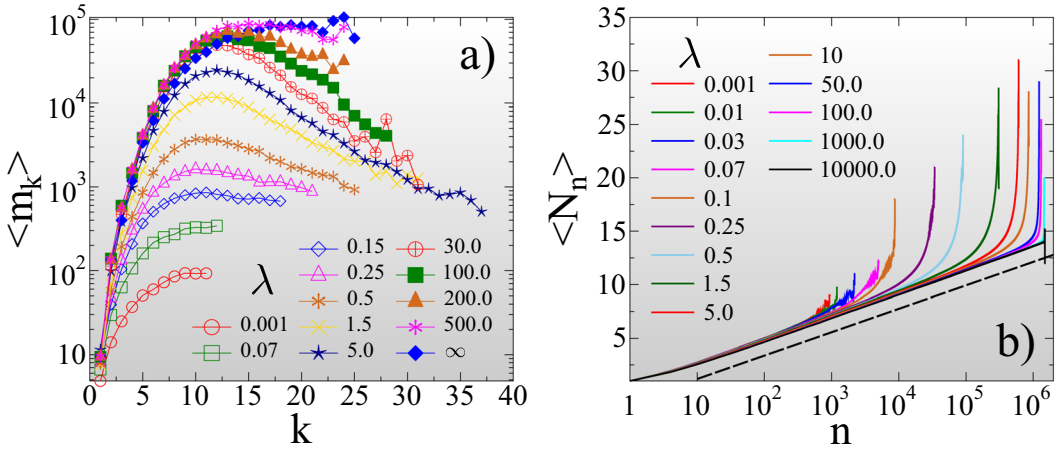

Figure 5. (**a**) Average lifetime of records $\langle m_k \rangle$ as a function of the record rank k for several values of the cutoff strength λ. (**b**) Average number of records $\langle N_n \rangle$ formed during the fracture process as a function of the event number n varying λ in a broad range. The value of the disorder exponent is fixed to $\mu = 0.7$. (GLE 4.2.5, http://glx.sourceforge.net/).

Approaching failure through accelerated record breaking. Inside the quasi-brittle phase, when the amount of disorder is reduced by the finite cutoff strength ε_{max} of fibers, the evolution of burst sequences substantially changes since the initial stationary regime is followed by acceleration in the vicinity of failure (see Fig. 2(a)). To facilitate the comparison of results obtained varying the cutoff strength ε_{max} at different exponents μ, we introduce the parameter $\lambda = (\varepsilon_{max} - \varepsilon^c_{max})/\varepsilon^c_{max}$, which characterizes the relative distance $\lambda > 0$ of the system from the phase boundary $\varepsilon^c_{max}(\mu)$ at a given value of μ. In order to determine how the precise amount of disorder controls the onset and significance of acceleration, and hence, the forecastability of ultimate failure, we performed computer simulations varying the value of λ and the disorder exponent μ in broad ranges $0.001 \leq \lambda \leq +\infty$ and $0.01 \leq \mu \leq 1$, respectively. At each parameter set averages were calculated over 6000 samples (for details of averaging see Methods).

Of course, the average size of records $\langle \Delta^k_r \rangle$ has the same monotonically increasing trend with the record rank k as in the ductile phase for all values of λ and μ (see SI4 for figure). However, the average lifetime of records $\langle m_k \rangle$ exhibits an astonishing behavior: As a representative example, Fig. 5(a) demonstrates for $\mu = 0.7$ that for a sufficiently high disorder $\lambda > 0.1$ the $\langle m_k \rangle$ curves develop a maximum at a characteristic record rank k^*. For low rank records $k < k^*$ the RB process slows down due to the stationarity of the beginning of the fracture process, while beyond the maximum $k > k^*$, the decreasing lifetime indicates that the approach to failure is accompanied by an accelerated record breaking. Note that as the amount of disorder grows with increasing λ, the position of the maximum k^* slightly shifts to higher values, while the maximum gets gradually less pronounced and eventually disappears when approaching ductile fracture.

Surprisingly, in the opposite limit $\lambda \to 0$ of low disorder, a similar behavior is observed: the record lifetime $\langle m_k \rangle$ tends to a monotonically increasing form showing the slowdown of record breaking, in spite of the rapid collapse of the highly brittle system.

The acceleration of the RB process results in a rapid increase of the number N_n of records close to failure. Figure 5(b) shows that at early stages of the fracture process the average record number $\langle N_n \rangle$ increases logarithmically with the number of bursts n in agreement with Eq. 4, however, at a characteristic event index n_{k^*}, corresponding approximately to the rank k^* of maximum lifetime, the functional form of $\langle N_n \rangle$ changes to a rapid increase. It is important to emphasize that varying the amount of disorder by λ, as the accelerating regime diminishes in the limits of highly brittle ($\lambda \to 0$) and ductile ($\lambda \to +\infty$) fracture, the deviations from the generic logarithmic trend of IIDs gradually disappear apart from some fluctuations.

Also the overall statistics of record sizes and lifetimes is sensitive to the degree of disorder. Figure 6(a) shows that close to the phase boundary of perfect brittleness $\lambda \to 0$ the size distribution of records $p(\Delta_r)$ is identical with the corresponding distribution of ductile fracture (see Fig. 4(c) for comparison), i.e. a power law distribution Eq. 7 is obtained with a universal exponent $\tau_r = 1$. Further from the phase boundary, the change in the dynamics of fracture from a steady evolution to acceleration gives rise to a crossover of $p(\Delta_r)$ between two regimes of different functional forms: for small records, generated during early stages of the fracture process, the distribution remains similar to its ductile counterpart, however, beyond a characteristic record size a steeper power law is formed. Simulations revealed that the crossover point practically coincides with the average record size $\langle \Delta^k_r \rangle$ at the rank k^* of the maximum lifetime in Fig. 5(a). The underlying mechanism of the emergence of the crossover of the distribution of record sizes is the crossover of the entire burst size distribution[69], similar to the so-called b-value anomaly observed for event magnitude distributions in geosystems[32,70,71].

The lifetime distribution $p(m)$ shows the same qualitative behavior as λ is varied. For clarity, the distributions $p(m)$ are presented separately for the parameter ranges where the acceleration of record breaking is absent and present, in Fig. 6(b,c), respectively. At low and high disorder, where no acceleration occurs, the waiting time

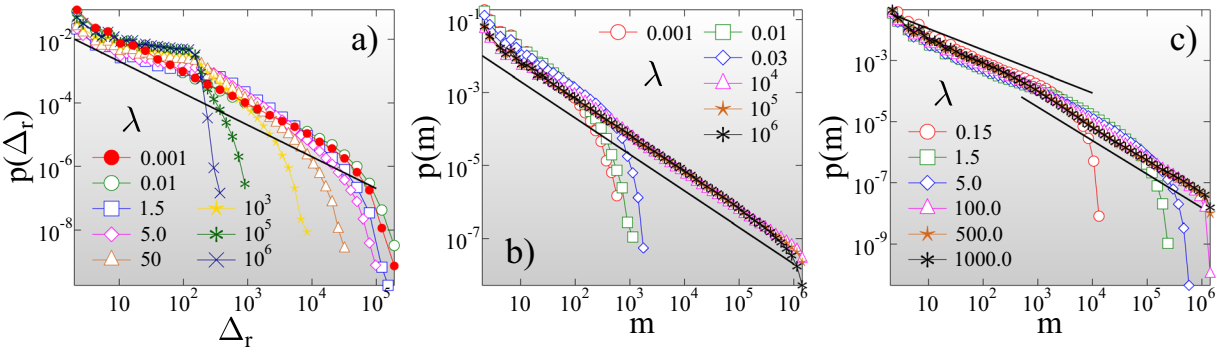

Figure 6. (**a**) Size distribution of record events $p(\Delta_r)$ for several values of λ. The straight line represents a power law of exponent $\tau_r = 1$. (**b**) Probability distribution of the lifetime of records $p(m)$ for cutoff strengths of fibers λ where the average waiting time in Fig. 5, (**b**) solely exhibits slowdown. The straight line represents a power law of exponent $z = 1$. (**c**) Lifetime distributions $p(m)$ for intermediate λ values where the RB process accelerates prior to failure. The two straight lines represent power laws of exponent $z_{a1} = 0.7$ and $z_{a2} = 1.15$. The disorder exponent μ has the same value $\mu = 0.7$ in the figures. (GLE 4.2.5, http://glx.sourceforge.net/).

distributions are consistent with the IID behavior Eq. 6 (Fig. 6(b)). For intermediate λ, when accelerated record breaking emerges, $p(m)$ exhibits a crossover between two power laws of different exponents (Fig. 6(c)). For short lifetimes, typical for the vicinity of failure, the exponent z_{a1} is smaller $z_{a1} = 0.7$, while, for large waiting times characteristic for the initial slowdown of the process, the exponent is higher $z_{a2} = 1.15$ than the IID result $z = 1$. It can be observed in Fig. 6(b,c) that the particular value of λ inside the two regimes only affects the crossover point and the cutoff of the distributions.

Simulations revealed that varying the disorder exponent μ the qualitative behaviour of the average waiting time $\langle m_k \rangle$ and event number $\langle N_n \rangle$, and of the distributions of record sizes $p(\Delta_r)$ and lifetimes $p(m)$, remains the same, they undergo only quantitative changes what we analyze in the next section. The results demonstrate that the statistics of records is very sensitive to the details of the crackling sequence providing a powerful tool to identify the onset of acceleration towards failure. Additionally, comparing the results to IID event sequences, our analysis proves that before acceleration the precursory bursting activity is dominated by the microscale disorder giving rise to stationarity. Acceleration starts when the stress enhancements generated by the redistribution of load after breaking bursts, can enhance the triggering of further avalanches.

The Effect of Disorder on the Onset of Acceleration

The presence of a sufficiently broad accelerating regime in the series of crackling events is of ultimate importance to obtain an early warning of the imminent failure and to forecast the final collapse of the evolving system with a good precision. The position of the maximum k^* of the average record lifetime $\langle m_k \rangle$ and the corresponding event index n_{k^*} provide an excellent signal of the start of acceleration towards failure after a longer period of stationary evolution. However, it can be observed in Fig. 5(a) that both the extension of the accelerating regime and the magnitude of acceleration depend on the degree of disorder in the system. To assess the predictability of the ultimate failure, the significance of the acceleration regime has to be characterized.

To quantify the extension of the accelerating regime we determined the difference δk of the highest record rank k_{max} obtained up to failure and the position of the maximum k^* of the record lifetimes in single samples. The average of this quantity

$$\langle \delta k \rangle = \langle k_{max} - k^* \rangle \tag{8}$$

over a large number of simulations is presented in Fig. 7(a) as a function of λ for several values of the disorder exponent μ. For each value of μ a well defined range of the cutoff strength λ can be identified where a significant difference $\langle \delta k \rangle > 1$ emerges between k^* and k_{max}. Both for a high degree of brittleness $\lambda \to 0$ and for ductile breaking $\lambda \to +\infty$, the value of $\langle \delta k \rangle$ is practically zero, which shows that no acceleration can be detected. Increasing the amount of disorder by decreasing the exponent μ, the acceleration regime $\langle \delta k \rangle > 1$ extends to higher values of the cutoff strength λ.

The magnitude of acceleration of the RB process can be characterized by comparing the last record lifetime $m_{k_{max}}$ and the maximum lifetime of records m_{k^*}. Figure 7(b) presents the average values $\langle m_{k_{max}} \rangle$ and $\langle m_{k^*} \rangle$, using the same scale of λ on the horizontal axis as in Fig. 7(a) to facilitate the comparison with the behavior of $\langle \delta k \rangle$. In the vicinity of $\mu = 1$ the two quantities $\langle m_{k_{max}} \rangle$ and $\langle m_{k^*} \rangle$ practically coincide for all values of the cutoff strength λ. However, lowering the exponent μ, a broader and broader range of λ emerges where a significant difference $\langle m_{k^*} \rangle \gg \langle m_{k_{max}} \rangle$ is obtained, indicating the presence of a dominating maximum of the record lifetime. The λ window of $\langle \delta k \rangle > 1$ coincides with that of $\langle m_{k^*} \rangle \gg \langle m_{k_{max}} \rangle$ verifying the existence of a well defined range of disorder where failure can be foreseen. Outside this window the degree of disorder is either too low or too high so that no signal of the imminent failure can be identified. This λ window of significant acceleration is highlighted by the vertical dashed lines in Fig. 7(a,b) for $\mu = 0.9$.

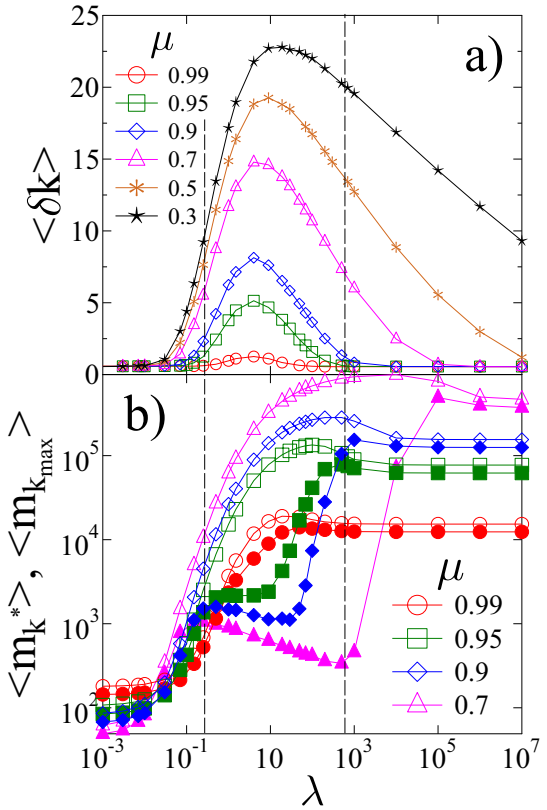

Figure 7. (**a**) Average value of the difference $\langle \delta k \rangle$ of the highest record rank k_{max} and the position of the maximum k^* of the record lifetime as a function of λ for several values of the disorder exponent μ. (**b**) The average of the maximum lifetime $\langle m_{k^*} \rangle$ (open symbols) and the lifetime of the last record $\langle m_{k_{max}} \rangle$ (filled symbols) as a function of λ. For clarity, pair of curves are presented only for four values of the disorder exponent μ. The vertical dashed lines indicate the λ window of acceleration for $\mu = 0.9$. (GLE 4.2.5, http://glx.sourceforge.net/).

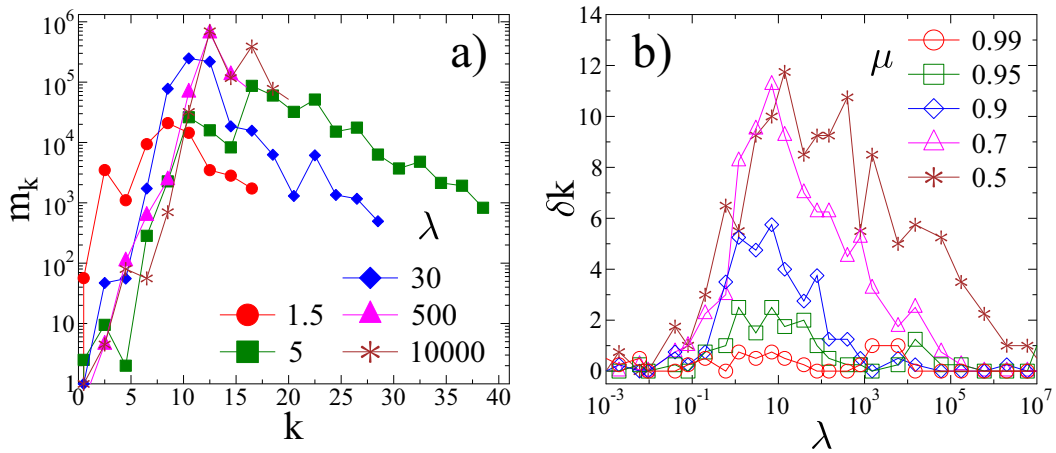

Figure 8. (**a**) The lifetime of consecutive records m_k, obtained during the evolution of a single system, as a function of their rank k for several values of λ at the same disorder exponent $\mu = 0.7$ as in Fig. 5 (**a**) for the sample averaged curves. (**b**) The difference δk of the highest record rank k_{max} and the position of the maximum k^* of the record lifetime for a single sample as a function of λ for several values of the disorder exponent μ. (GLE 4.2.5, http://glx.sourceforge.net/).

For the practical applications of record statistics to determine the start of the critical regime of the dynamics, the method has to provide reliable results for single samples. Figure 8(a) presents the lifetime of consecutive records m_k as a function of their rank k obtained by the analysis of a single system for several values of λ at the same disorder exponent $\mu = 0.7$ as in Fig. 5(a). It is important to emphasize that apart from fluctuations records

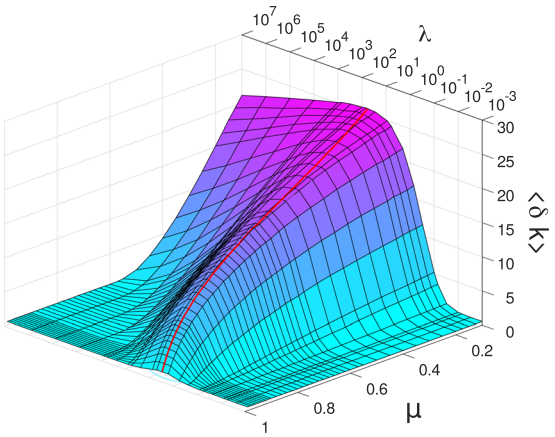

Figure 9. Three-dimensional representation of the $\langle \delta k(\mu, \lambda) \rangle$ function, which gives an overview of the forecastability of failure in terms of disorder. The bold red line highlights the ridge of the surface, where the broadest acceleration regime is obtained. (MATLAB 2018a, https://uk.mathworks.com/).

of the single sample exhibit the same overall behaviour as the sample averaged curves in Fig. 5(a), i.e. m_k has a well defined maximum in the quasi brittle regime of the fracture process so that the value of the record rank k^* and the corresponding event index n_{k^*} can be obtained in a reliable way. This result is further supported by the behaviour of δk in Fig. 8(b) which shows that the window of forecastability of a single system, where a significant accelerating regime can be detected by the method of record statistics, agrees very well with the sample averaged result of Fig. 7(a). Simulations showed that the relative value of sample-to-sample fluctuations of record quantities vary between 0.05 and 0.2, typically increasing with the record rank k, making the method efficient for single samples undergoing quasi-brittle fracture.

Discussion

Catastrophic failure of engineering constructions and of geosystems is often caused by the fracture of disordered materials. Under a constant or slowly varying external load, the inherent disorder of materials gives rise to a jerky evolution of the fracture process accompanied by a sequence of acoustic outbreaks. Methods of failure forecasting predict the lifetime of the evolving system by exploiting the power law acceleration of the precursory crackling activity prior to ultimate failure. Here we focused on the acceleration preceding the final collapse, and proposed a method to identify the onset of this critical regime of the dynamics which can be used as an early warning of the imminent failure. Based on a fiber bundle model of fracture phenomena, we studied the statistics of record size events to reveal how the sequence of breaking bursts evolves as the system approaches failure. We demonstrated that the small subset of record bursts grasps essential features of the dynamics leading to ultimate failure, with the additional advantage that they are relatively easy to identify even experimentally over the noisy background.

As an important outcome of the work, we showed that during quasi-brittle fracture, where failure proceeds through an intense precursory activity, the acceleration of the crackling sequence towards failure is accompanied by an accelerated record breaking. The onset of acceleration can be identified by the record which has the longest lifetime so that its rank k^*, and the corresponding event index n_{k^*} provide a reliable signal in the burst sequence where the critical regime of the dynamics starts. Before this characteristic record, the process of record breaking slows down and the statistics of records proved to be equivalent with the behavior of event sequences of IIDs. These results imply that the beginning of fracture is dominated by the disorder of the material in spite of the increasing external load and decreasing load bearing capacity of the system. Beyond k^*, acceleration is caused by the enhanced triggering of bursts following the stress redistribution after breaking events.

Early warning and forecastability of the imminent failure requires a sufficiently broad critical regime with a considerable magnitude of acceleration. To asses the effect of disorder on the forecastability of failure, we made a quantitative characterization of the significance of acceleration in terms of record statistics. Most notably, we showed that the highly brittle fracture of low disorder materials, and the ductile failure of the strongly disordered ones, are both unpredictable. In spite of the considerable number of bursts generated, the absence of acceleration limits forecastability to a well defined range of disorder on the phase diagram of the system. This is illustrated in Fig. 9 which presents the value of $\langle \delta k \rangle$ over the $\mu - \lambda$ plane. It can be observed that for the significance of the accelerating regime, disorder has an optimum amount, i.e. the combination of the disorder exponent μ and of the cutoff strength λ of fibers determining the ridge of the $\langle \delta k \rangle$ surface provides the best predictability. Note that lowering the exponent μ results in a broadening of the λ range where a significant acceleration occurs so that the range of predictability tends to infinity in terms of λ for $\mu \to 0$. Our results imply that former conclusions in the literature that increasing disorder improves forecastability is generally not valid for fat-tailed disorder. Increasing the cutoff strength λ beyond the ridge of $\langle \delta k \rangle(\mu, \lambda)$ at fixed exponents μ in Fig. 9, disorder becomes disadvantageous. The absolute upper bound of predictability is defined by the line on the $\mu - \lambda$ plane, where $\langle \delta k \rangle \approx 0$ holds in the high λ regime (see Fig. 9). This bound emerges due to the slow decay of the fat-tailed threshold distribution: since the tail of the strength distribution Eq. 1 is efficiently sampled even at small system sizes, at sufficiently

high upper cutoffs λ there will be so strong fibers in the system which can stabilize the fracture process till the end. As a consequence, ductile behaviour can already be reached at finite λ values. Predictability has also a lower bound which extends from $\lambda \approx 0.01$ to $\lambda \approx 0.1$ as μ increases from 0 to 1 (see Fig. 9).

To analyze the evolution of the failure process, we only considered the magnitude of crackling events. The RB analysis is similar to the natural time analysis in the sense that the physical time of events is ignored and only the magnitude of events is considered as a function of their order parameter. For practical applications, the adaptation of our method is straightforward in those cases, where the system approaches failure through an increasing activity of acoustic or seismic events. Laboratory experiments have revealed an accelerating rate of acoustic events accompanied by an increasing average event magnitude during the tertiary regime of the creep failure of heterogeneous materials[5,13,63–65], and for the approach to failure of porous rocks under a slowly increasing compressive load[12,16,30,34]. A similar behaviour of the rate of acoustic or seismic signals has been observed for the failure of geosystems such as volcanic eruptions[8,66], cliff collapses[21], the breakoff of hanging glaciers[67], and in some cases also for landslides[23,33]. In these systems, records either of the fluctuating daily (hourly) rate of seismic (acoustic) events, or of the magnitude of individual signals can serve as the starting point of the analysis of record statistics. After setting the first record of the time window of the analysis, the rest of the record events can be unambigously identified since the largest events of the sequence have to be found. Our method suggests that the event index n_{k^*} of the longest living record, and its corresponding physical time, provide the onset of acceleration of the record breaking process, and hence, of the start of the critical regime of the approach to failure. Failure forecast methods (FFM) predict the time of failure based on the power law acceleration of a characteristic quantity of the time evolution of the system. Our method can also be used to complement FFMs by conditioning a series of discrete events to identify the time window where the assumption of a power law acceleration is applicable[1,3].

Our study is based on a fiber bundle model with equal load sharing which is essentially a mean field approach to fracture. The model has the advantage that solely one source of disorder is present in the system, i.e. the random strength of fibers. In more realistic situations stress fluctuations occur around cracks. Recently, we have shown in ref. [60] that when the strength disorder is very high in the system with fat-tailed local strength distributions, stress concentration around cracks have a minor effect on the breakdown process. Hence, we conjecture that our statements have a broader validity, they are not limited by the assumption of the homogeneous stress field.

Methods

To study the fracture of heterogeneous materials we use a fiber bundle model which provides a straightforward way to reveal the role of microscale disorder in fracturing. The model is composed of N parallel fibers with a perfectly brittle response, i.e. the fibers exhibit a linearly elastic behavior up to breaking at a critical deformation ε_{th}. Materials' disorder is introduced by the random strength of fibers $\varepsilon_{th}^{i} (i = 1, \ldots, N)$ for which we considered a power law distribution over a finite range. Computer simulations were performed by slowly increasing the external load on the bundle to provoke the breaking of a single fiber. The load of broken fibers is overtaken by the remaining intact ones. We assume equal load sharing after breaking events which ensures that all fibers keep the same load during the entire breaking process. Since no stress fluctuations can arise, the random strength of fibers is the only source of disorder in the system.

After load redistribution, the excess load may trigger additional breakings, which is again followed by load redistribution. Eventually, such repeated cycles of breaking and load redistribution steps give rise to bursts of breakings in the model which are analogous to the acoustic outbreaks of real experiments. The size of bursts Δ is defined as the number of fibers breaking in the avalanche. In all the simulations presented in the manuscript the number of fibers was fixed $N = 5 \times 10^6$ and averaging was performed over 6000 samples, which provided a sufficient precision for the data analysis.

Characteristic quantities of records such as the average size $\langle \Delta_r^k \rangle$ and lifetime $\langle m_k \rangle$ were obtained by averaging over the samples at fixed record ranks k. The same type of sample average was calculated for the average number of records $\langle N_n \rangle$ and $\langle \delta k \rangle$ at fixed event numbers n and upper cutoffs λ, respectively. Probability densities $p(\Delta_r)$ and $p(m)$ were obtained for the entire ensemble of samples at given values of the control parameters μ and λ.

Received: 11 October 2019; Accepted: 22 January 2020;
Published online: 13 February 2020

References

1. Voight, B. A method for prediction of volcanic eruptions. *Nature* **332**, 125–130 (1988).
2. Voight, B. A Relation to Describe Rate-Dependent Material Failure. *Science* **243**, 200–203 (1989).
3. Main, I. G. Applicability of time-to-failure analysis to accelerated strain before earthquakes and volcanic eruptions. *Geophys. J. Int.* **139**, F1–F6 (1999).
4. Turcotte, D. L., Newman, W. I. & Shcherbakov, R. Micro and macroscopic models of rock fracture. *Geophys. J. Int.* **152**, 718 (2003).
5. Koivisto, J., Ovaska, M., Miksic, A., Laurson, L. & Alava, M. J. Predicting sample lifetimes in creep fracture of heterogeneous materials. *Phys. Rev. E* **94**, 023002 (2016).
6. Pradhan, S., Kjellstadli, J. T. & Hansen, A. Variation of elastic energy shows reliable signal of upcoming catastrophic failure. *Front. Phys.* **7**, 106 (2019).
7. Tárraga, M., Carniel, R., Ortiz, R. & García, A. Chapter 13 the failure forecast method: Review and application for the real-time detection of precursory patterns at reawakening volcanoes. In Gottsmann, J. & Marti, J. (eds.) *Caldera Volcanism: Analysis, Modelling and Response*, vol. 10 of *Developments in Volcanology*, 447 – 469 (Elsevier, 2008).
8. Bell, A. F., Greenhough, J., Heap, M. J. & Main, I. G. Challenges for forecasting based on accelerating rates of earthquakes at volcanoes and laboratory analogues. *Geophys. J. Int.* **185**, 718–723 (2011).
9. Dahmen, K. A., Ben-Zion, Y. & Uhl, J. T. A simple analytic theory for the statistics of avalanches in sheared granular materials. *Nat. Phys.* **7**, 554–557 (2011).
10. Baró, J. *et al.* Statistical similarity between the compression of a porous material and earthquakes. *Phys. Rev. Lett.* **110**, 088702 (2013).
11. Salje, E. K. & Dahmen, K. A. Crackling Noise in Disordered Materials. *Annu. Rev. Condens. Matter Phys.* **5**, 233–254 (2014).
12. Nataf, G. F. *et al.* Predicting failure: acoustic emission of berlinite under compression. *J. Physics: Condens. Matter* **26**, 275401 (2014).

13. Guarino, A., Garcimartin, A. & Ciliberto, S. An experimental test of the critical behaviour of fracture precursors. *Eur. Phys. J. B* **6**, 13–24 (1998).
14. Rosti, J., Illa, X., Koivisto, J. & Alava, M. J. Crackling noise and its dynamics in fracture of disordered media. *J. Phys. D: Appl. Phys.* **42**, 214013 (2009).
15. Hao, S.-W. *et al*. Power-law singularity as a possible catastrophe warning observed in rock experiments. *Int. J. Rock Mech. Min. Sci.* **60**, 253–262 (2013).
16. Vasseur, J. *et al*. Heterogeneity: The key to failure forecasting. *Sci. Rep.* **5**, 13259 (2015).
17. Pradhan, S., Hansen, A. & Hemmer, P. C. Crossover behavior in burst avalanches: Signature of imminent failure. *Phys. Rev. Lett.* **95**, 125501 (2005).
18. Johansen, A. & Sornette, D. Critical ruptures. *Eur. Phys. J. B* **18**, 163–181 (2000).
19. Uyeda, S., Nagao, T., Orihara, Y., Yamaguchi, T. & Takahashi, I. Geoelectric potential changes: Possible precursors to earthquakes in Japan. *Proc. Natl. Acad. Sci. USA* **97**, 4561–4566 (2000).
20. Heap, M. *et al*. Brittle creep in basalt and its application to time-dependent volcano deformation. *Earth Planet. Sci. Lett.* **307**, 71–82 (2011).
21. Amitrano, D., Grasso, J. R. & SenfauteG. Seismic precursory patterns before a cliff collapse and critical point phenomena. *Geophys. Res. Lett*., **32** (2005).
22. Amitrano, D. & Helmstetter, A. Brittle creep, damage, and time to failure in rocks. *J. Geophys. Res. Solid Earth*, **111** (2006).
23. Michlmayr, G., Chalari, A., Clarke, A. & Or, D. Fiber-optic high-resolution acoustic emission (AE) monitoring of slope failure. *Landslides* **14**, 1139–1146 (2017).
24. Sarlis, N. V., Skordas, E. S., Lazaridou, M. S. & Varotsos, P. A. Investigation of seismicity after the initiation of a Seismic Electric Signal activity until the main shock. *Proc. Jpn. Acad. Ser. B Phys. Biol. Sci.* **84**, 331–343 (2008).
25. Varotsos, P. A., Sarlis, N. V. & Skordas, E. S. Scale-specific order parameter fluctuations of seismicity in natural time before mainshocks. *EPL (Europhysics Lett.)* **96**, 59002 (2011).
26. Sarlis, N., Skordas, E. & Varotsos, P. The change of the entropy in natural time under time-reversal in the olami-feder-christensen earthquake model. *Tectonophysics* **513**, 49–53 (2011).
27. Sarlis, N. V., Skordas, E. S. & Varotsos, P. A. A remarkable change of the entropy of seismicity in natural time under time reversal before the super-giant m9 tohoku earthquake on 11 march 2011. *EPL (Europhysics Lett.)* **124**, 29001 (2018).
28. Varotsos, P. A., Sarlis, N. V., Skordas, E. S., Christopoulos, S.-R. G. & Lazaridou-Varotsos, M. S. Identifying the occurrence time of an impending mainshock: a very recent case. *Earthq Sci.* **28**, 215–222 (2015).
29. de Blasio, F. V.*Introduction to the Physics of Landslides* (Springer Verlag, Heidelberg, 2011).
30. Xu, Y., Borrego, A. G., Planes, A., Ding, X. & Vives, E. Criticality in failure under compression: Acoustic emission study of coal and charcoal with different microstructures. *Phys. Rev. E* **99**, 033001 (2019).
31. Andersen, J. V. & Sornette, D. Predicting failure using conditioning on damage history: Demonstration on percolation and hierarchical fiber bundles. *Phys. Rev. E* **72**, 056124 (2005).
32. Sammonds, P. R., Meredith, P. G. & Main, I. G. Role of pore fluids in the generation of seismic precursors to shear fracture. *Nature* **359**, 228–230 (1992).
33. Sammonds, P. & Ohnaka, M. Evolution of microseismicity during frictional sliding. *Geophys. Res. Lett.* **25**, 699–702 (1998).
34. Baró, J. *et al*. Experimental evidence of accelerated seismic release without critical failure in acoustic emissions of compressed nanoporous materials. *Phys. Rev. Lett.* **120**, 245501 (2018).
35. Petri, A., Paparo, G., Vespignani, A., Alippi, A. & Costantini, M. Experimental evidence for critical dynamics in microfracturing processes. *Phys. Rev. Lett.* **73**, 3423 (1994).
36. Hao, S., Liu, C., Lu, C. & Elsworth, D. A relation to predict the failure of materials and potential application to volcanic eruptions and landslides. *Sci. Reports* **6**, 27877 (2016).
37. Brechet, Y., Magnin, T. & Sornette, D. The coffin-manson law as a consequence of the statistical nature of the LCF surface damage. *Acta Metall. et Materialia* **40**, 2281–2287 (1992).
38. Zapperi, S., Ray, P., Stanley, H. E. & Vespignani, A. First-Order transition in the breakdown of disordered media. *Phys. Rev. Lett.* **78**, 1408 (1997).
39. Sornette, D. & Andersen, J. Scaling with respect to disorder in time-to-failure. *Eur. Phys. J. B* **1**, 353 (1998).
40. Menezes-Sobrinho, I. & Rodrigues, A. Influence of disorder on the rupture process of fibrous materials. *Phys. A: Stat. Mech. its Appl.* **389**, 5581–5586 (2010).
41. Ramos, O., Cortet, P.-P., Ciliberto, S. & Vanel, L. Experimental study of the effect of disorder on subcritical crack growth dynamics. *Phys. Rev. Lett.* **110**, 165506 (2013).
42. Sornette, D. Predictability of catastrophic events: Material rupture, earthquakes, turbulence, financial crashes, and human birth. *Proc. Natl. Acad. Sci. USA* **99**, 2522–2529 (2002).
43. Saichev, A. & Sornette, D. Andrade, omori and time-to-failure laws from thermal noise in material rupture. *Phys. Rev. E* **71**, 016608 (2005).
44. Varotsos, P. A., Sarlis, N. V., Skordas, E. S. & Lazaridou, M. S. Identifying sudden cardiac death risk and specifying its occurrence time by analyzing electrocardiograms in natural time. *Appl. Phys. Lett.* **91**, 064106 (2007).
45. Sarlis, N. V., Skordas, E. S., Varotsos, P. A., Ramírez-Rojas, A. & Flores-Márquez, E. L. Natural time analysis: On the deadly mexico m8.2 earthquake on 7 september 2017. *Phys. A* **506**, 625–634 (2018).
46. Varotsos, P., Sarlis, N. V. & Skordas, E. S.*Natural Time Analysis: The New View of Time* (Springer-Verlag, Berlin, Heidelberg, Berlin, 2011), 1st edn.
47. Hansen, A., Hemmer, P. & Pradhan, S.*The Fiber Bundle Model: Modeling Failure in Materials*. Statistical Physics of Fracture and Breakdown (Wiley, 2015).
48. Kun, F., Raischel, F., Hidalgo, R.C. & Herrmann, H.J.Extensions of fiber bundle modelsInBhattacharyyaP. and ChakrabartiB.K.(eds.) Extensions of fiber bundle models. In Bhattacharyya, P. and Chakrabarti, B. K. (eds.) *Modelling Critical and Catastrophic Phenomena in Geoscience: A Statistical Physics Approach*, Lecture Notes in Physics, 57–92 (Springer-Verlag Berlin Heidelberg New York, 2006).
49. Hidalgo, R. C., Kun, F. & Kovács, K. and Pagonabarraga, I. Avalanche dynamics of fiber bundle models. *Phys. Rev. E* **80**, 051108 (2009).
50. Wergen, G. & Krug, J. Record-breaking temperatures reveal a warming climate. *Europhys. Lett.* **92**, 30008 (2010).
51. Davidsen, J., Grassberger, P. & Paczuski, M. Earthquake recurrence as a record breaking process. *Geophys. Res. Lett*.**33** (2006). L11304.
52. Davidsen, J., Grassberger, P. & Paczuski, M. Networks of recurrent events, a theory of records, and an application to finding causal signatures in seismicity. *Phys. Rev. E* **77**, 066104 (2008).
53. Yoder, M. R., Turcotte, D. L. & Rundle, J. B. Record-breaking earthquake intervals in a global catalogue and an aftershock sequence. *Nonlin. Proc. Geophys.* **17**, 169–176 (2010).
54. Miller, P. W. & Ben-Naim, E. Scaling exponent for incremental records. *J. Stat. Mech.: Theor. Exp.* **2013**, P10025 (2013).
55. Wergen, G. Records in stochastic processes-"theory and applications. *J. Phys. A: Math. Theor.* **46**, 223001 (2013).
56. Shcherbakov, R., Davidsen, J. & Tiampo, K. F. Record-breaking avalanches in driven threshold systems. *Phys. Rev. E* **87**, 052811 (2013).
57. Danku, Z. & Kun, F. Record breaking bursts in a fiber bundle model of creep rupture. *Front. Phys.* **2**, 8 (2014).

58. Pál, G., Raischel, F., Lennartz-Sassinek, S., Kun, F. & Main, I. G. Record-breaking events during the compressive failure of porous materials. *Phys. Rev. E* **93**, 033006 (2016).
59. Majumdar, S. N., vonBomhard, P. & Krug, J. Exactly solvable record model for rainfall. *Phys. Rev. Lett.* **122**, 158702, https://doi.org/10.1103/PhysRevLett.122.158702 (2019).
60. Danku, Z. & Kun, F. Fracture process of a fiber bundle with strong disorder. *J. Stat. Mech.: Theor. Exp.* **2016**, 073211 (2016).
61. Kádár, V., Danku, Z. & Kun, F. Size scaling of failure strength with fat-tailed disorder in a fiber bundle model. *Phys. Rev. E* **96**, 033001 (2017).
62. Sarlis, N. V., Skordas, E. S. & Varotsos, P. A. Heart rate variability in natural time and 1/f "noise". *EPL (Europhysics Lett.)* **87**, 18003 (2009).
63. Garcimartin, A., Guarino, A., Bellon, L. & Ciliberto, S. Statistical properties of fracture precursors. *Phys. Rev. Lett.* **79**, 3202 (1997).
64. Nechad, H., Helmstetter, A., Guerjouma, R. E. & Sornette, D. Creep ruptures in heterogeneous materials. *Phys. Rev. Lett.* **94**, 045501 (2005).
65. Rosti, J., Koivisto, J. & Alava, M. J. Statistics of acoustic emission in paper fracture: precursors and criticality. *J. Stat. Mech.* **2010**, P02016 (2010).
66. Bell, A. F., Naylor, M. & Main, I. G. The limits of predictability of volcanic eruptions from accelerating rates of earthquakes. *Geophys. J. Int.* **194**, 1541–1553 (2013).
67. Faillettaz, J., Pralong, A., Funk, M. & Deichmann, N. Evidence of log-periodic oscillations and increasing icequake activity during the breaking-off of large ice masses. *J. Glaciol.* **54**, 725–737 (2008).
68. Gembris, D., Taylor, J. G. & Suter, D. Evolution of athletic records: Statistical effects versus real improvements. *J. Appl. Stat.* **34**, 529–545 (2007).
69. Kádár, V. & Kun, F. System-size-dependent avalanche statistics in the limit of high disorder. *Phys. Rev. E* **100**, 053001 (2019).
70. Amitrano, D. Variability in the power-law distributions of rupture events. *Eur. Phys. J. Special Top.* **205**, 199–215 (2012).
71. Amitrano, D. Brittle-ductile transition and associated seismicity: Experimental and numerical studies and relationship with the b-values. *J. Geophys. Res.* **108**, 2044 (2003).

Acknowledgements

The work is supported by the EFOP-3.6.1-16-2016-00022 project. The project is co-financed by the European Union and the European Social Fund. This research was supported by the National Research, Development and Innovation Fund of Hungary, financed under the K-16 funding scheme Project no. K 119967. The research was financed by the Higher Education Institutional Excellence Program of the Ministry of Human Capacities in Hungary, within the framework of the Energetics thematic program of the University of Debrecen. Open access funding provided by University of Debrecen.

Author contributions

V.K. carried out computer simulations. V.K., G.P. and F.K. performed the data analysis. F.K. conceived of and designed the study, and drafted the manuscript. All authors read and approved the manuscript.

Competing interests

The authors declare no competing financial interests.

Additional information

Supplementary information is available for this paper at https://doi.org/10.1038/s41598-020-59333-4.

Correspondence and requests for materials should be addressed to F.K.

Reprints and permissions information is available at www.nature.com/reprints.

Publisher's note Springer Nature remains neutral with regard to jurisdictional claims in published maps and institutional affiliations.